Circ J 2008; **72:** 94 – 101

Magnetic Dispersion of the Late Repolarization in Brugada Syndrome

Boyoung Joung, MD, PhD; Kiwoong Kim, PhD*; Yong-Ho Lee, PhD*;
Hyukchan Kwon, PhD*; Hyun Kyoon Lim, PhD*; Tae-Uen Kim*;
Young-Guk Ko, MD, PhD; Moonhyoung Lee, MD, PhD;
Namsik Chung, MD, PhD; Sungsoon Kim, MD, PhD

Background Magnetocardiography (MCG) is a new noninvasive modality for recording cardiac depolarization and repolarization and was used in the present study to evaluate abnormalities in patients with Brugada syndrome (BS).

Methods and Results The MCG findings of 10 BS, 21 right bundle branch block (RBBB), and 34 normal patients were compared. On the horizontal spatiotemporal activation graph (STAG), the r' waves were more frequently located on the right side in the RBBB than in the normal (p=0.001) or BS groups (p=0.001). The maximum current angles of the r' wave fell into the northwest axis in all BS patients as compared to having a right axis deviation in 19 of 21 RBBB patients (90.4%, p=0.001). In the magnetic field and current density vector maps during late repolarization, the BS group had a non-dipole pattern more frequently and a higher number of poles compared with the normal (p=0.001) and RBBB groups (p=0.001).

Conclusions During depolarization, the horizontal STAG location and maximum current angle of the r' wave were beneficial in differentiating BS from RBBB and normal. The magnetic dispersion was a more frequently observed finding in BS patients than in RBBB and normal patients during late repolarization. (*Circ J* 2008; **72:** 94 – 101)

Key Words: Brugada syndrome; Bundle branch block; Depolarization; Repolarization; Magnetic dispersion; Magnetocardiography

Brugada syndrome (BS) is an inherited arrhythmogenic disease characterized by a typical electrocardiographic (ECG) pattern with ST-segment elevation in leads V_1 through V_3, incomplete right bundle-branch block (RBBB), and an increased risk of sudden cardiac death because of ventricular fibrillation (VF)[1,2] According to a study of the cellular basis of BS, the heterogeneity of the repolarization across the ventricular wall (differences in the action potential duration) of the right ventricular outflow tract may be a cause of the ST-elevation and the genesis of ventricular tachycardia (VT)/VF[2–4] The diagnosis of BS is mainly dependent on the typical ECG pattern and clinical manifestations. A differential diagnosis is at times difficult, particularly when the degree of the ST-segment elevation is relatively small. Moreover, the ECG signature of BS is dynamic and often concealed.

Magnetocardiography (MCG) is reported to have the potential to obtain current distributions with a high spatial resolution and to provide more detailed information of ventricular depolarization and repolarization[5] Recently, a study of the MCG findings in BS reported that the electrical conduction rate to the posterosuperior septal area is low[6] However, whether MCG can provide greater diagnostic benefit for BS remains unclear, because the data on the MCG findings in BS are limited. In the present study, we analyzed the MCG characteristics associated with BS by comparing normal and RBBB patients using 64-channel MCG.

(Received May 7, 2007; revised manuscript received August 8, 2007; accepted September 21, 2007)
*Cardiology Division, Department of Internal Medicine, Yonsei University Medical College, Seoul, *Bio-signal Research Center, Korea Research Institute of Standards and Science, Daejeon, Korea*
Acknowledgement of all sources of financial support: nothing to reveal.
Mailing address: Boyoung Joung, MD, PhD, Division of Cardiology, Yonsei Cardiovascular Center, Yonsei University College of Medicine, 134 Shinchon-dong, Seodaemun-gu, Seoul 120-752, Korea. E-mail: cby6908@yumc.yonsei.ac.kr

Methods

Study Population

The study consisted of 10 BS (10 males, age: 36.9±10.4 years), 21 RBBB (16 males, age: 50.8±15.5 years) and 34 normal patients (31 males, age: 32.5±11.4 years). The BS group included 10 consecutive patients diagnosed with BS at the Yonsei Cardiovascular Center. The diagnosis of BS was based on the findings of a typical ECG pattern (persistent or transient ST-segment elevation in the right precordial leads with or without an atypical RBBB pattern) with or without any clinical arrhythmic events (syncope, VF, or cardiac arrest)[7] The clinical arrhythmic events were sudden cardiac death with VF in 5 BS patients, and syncope in 1 BS patient. The other 4 BS patients were asymptomatic without family history of syncope or sudden death. According to the first consensus on BS conducted in Europe[8] the ECGs in the BS patients are classified as either type I (n=6) or type II (n=4). None of the patients, including the RBBB and normal groups, had any structural heart disease or coronary disease.

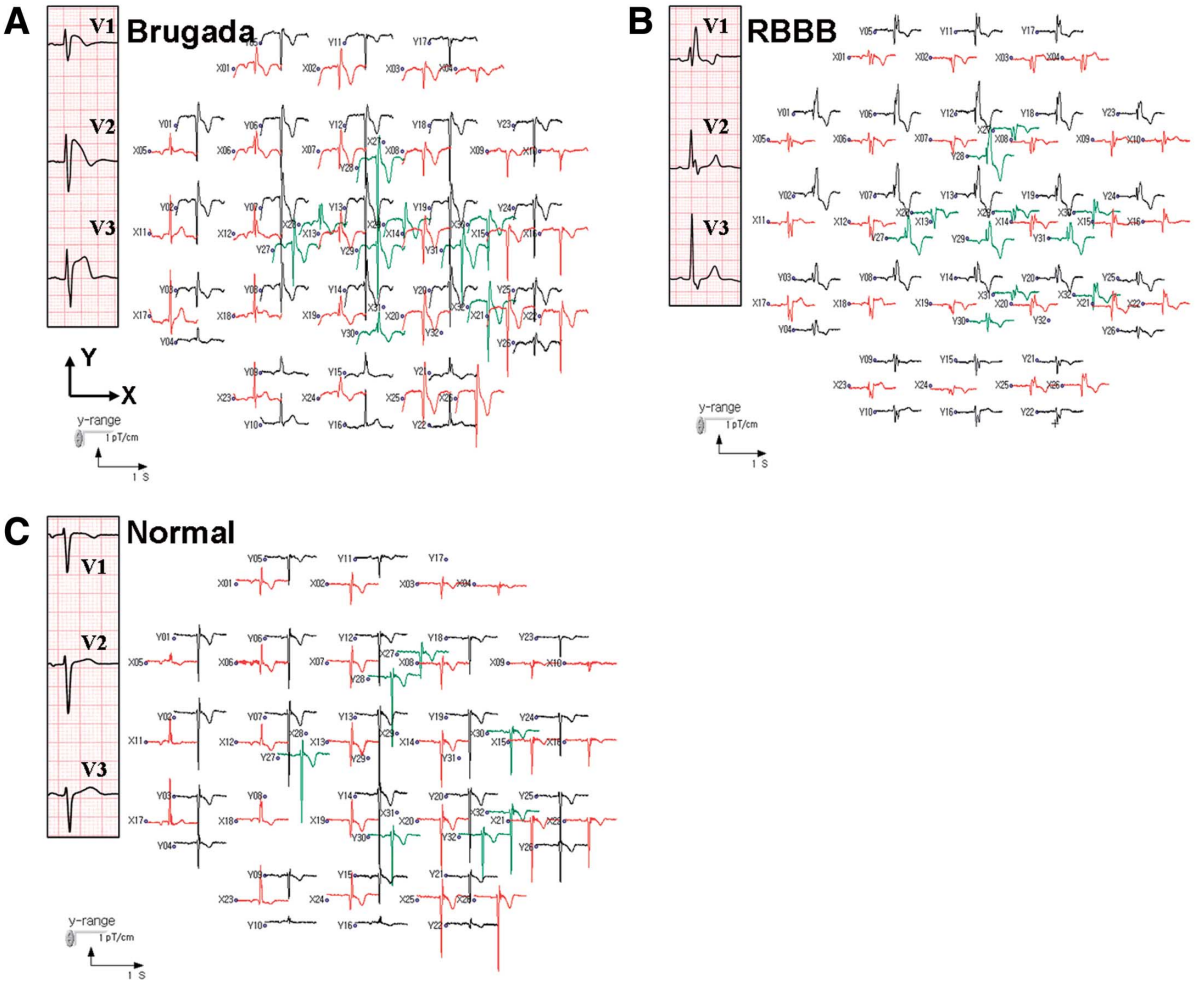

Fig 1. Representative electrocardiographics and corresponding magnetocardiography (MCG) time tracings. (A) Brugada syndrome, (B) right bundle branch block (RBBB), and (C) normal patient (see text for details).

MCG Recording and Interpretation

In all the subjects, 12-lead ECG and MCG were recorded within 30 min while at rest. The MCG recordings were performed using a KRISS 64-channel biomagnetometer (Bio-signal Research Center, KRISS, Daejeon, Korea) in a magnetically shielded room. The MCG system uses double relaxation oscillation SQUID (DROS) sensors[9,10] The average noise spectral density of the entire system in a magnetically shielded room is 10 fT/$\sqrt{\text{Hz}}$ at 1 Hz and 5 fT/$\sqrt{\text{Hz}}$ over 100 Hz. The KRISS 64-channel MCG has 64 planar first-order SQUID gradiometers, which measurd the tangential components of the cardiomagnetic fields. Typical recording time was 30 s. The MCG data for all the subjects were analyzed using application software, KRISSMCG64 (Bio-signal Research Center).

The interpretation of the MCG data was based on the MCG time tracings, spatiotemporal activation graph (STAG), magnetic field (MF) map and current density vector (CDV) map. The single beats from the raw data obtained from each subject were digitally averaged to reduce any noise. For each subject, an independent observer blindly examined the averaged data using a fixed time window (1.0 s) and signal gain within defined limits (0.5–2.0 pT/cm).

MCG Time Tracing and STAG

The MCG time tracing was the recording of the raw signal in 64 sites according to time (Fig 1). The integrated MCG time tracing was the summation of the raw signals from 64 recording sites. In the integrated MCG time tracings, the Q, R, and T waves and the QT interval were identified. If the R wave had 2 peaks, the first and second peaks (Rp, r'p) were analyzed separately. The end of the T wave (Te) was defined as the time of the visually determined vertex (maximum curvature) of the signal following the inflection point after the peak of the T wave (Tp). The average magnetic field strength of Rp, r'p and Tp in the integrated MCG time tracings was measured and compared among the 3 groups.

We created a longitudinal and horizontal STAG, which represented the time-dependent activation from the base to the apex and from left to right, respectively (Fig 2). In the longitudinal STAG, the relative location of the r' wave from the R wave was identified as the base, neutral, or apex. In the horizontal STAG, the relative location of the r' wave from the R wave was identified as right, neutral, or left. The STAG was created from depolarization to repolarization.

The CDV and MF Maps

The CDV map represents with arrows the amplitude and

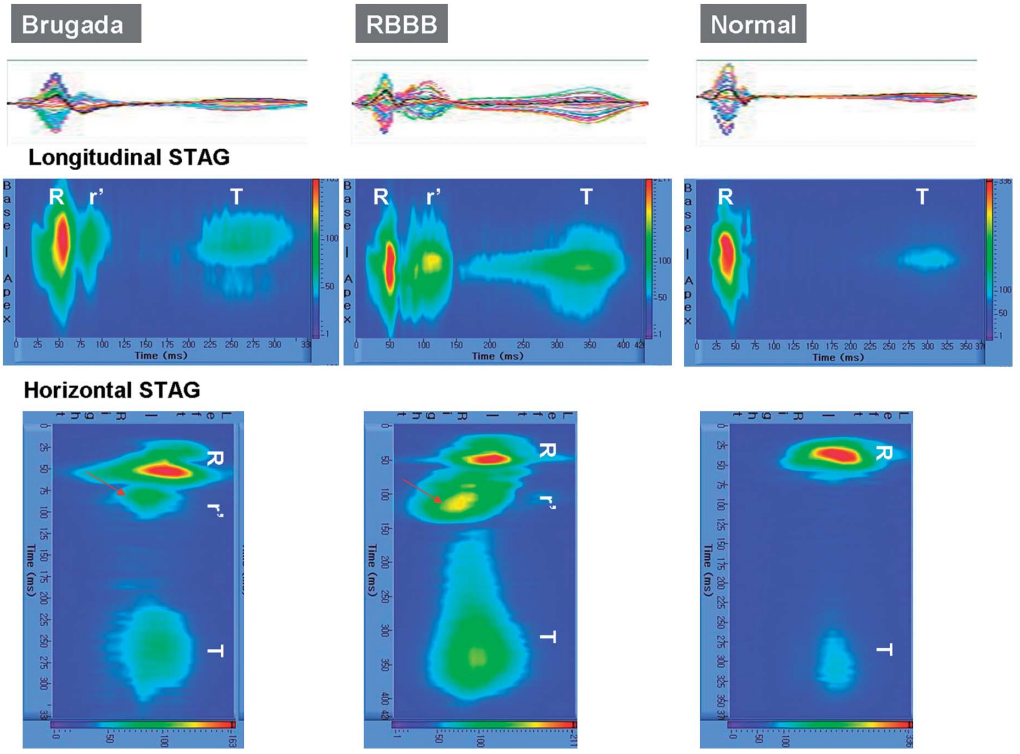

Fig 2. Comparison of the spatiotemporal activation graph (STAG) from depolarization to repolarization among the 3 groups. The upper, middle and lower panels in each diagram are the integrated magnetocardiography (MCG) time tracings, the longitudinal STAG, and the horizontal STAG, respectively. As in the MCG time tracings, the activation of the r' was more prominent in the right bundle branch block (RBBB) group than in the normal group. In the horizontal STAG, the r' activation of the Brugada syndrome and RBBB patients fell on the neutral and right side, respectively (arrows in left and middle lower panels). The r' activation of the normal patient was too small to interpret (right lower panel).

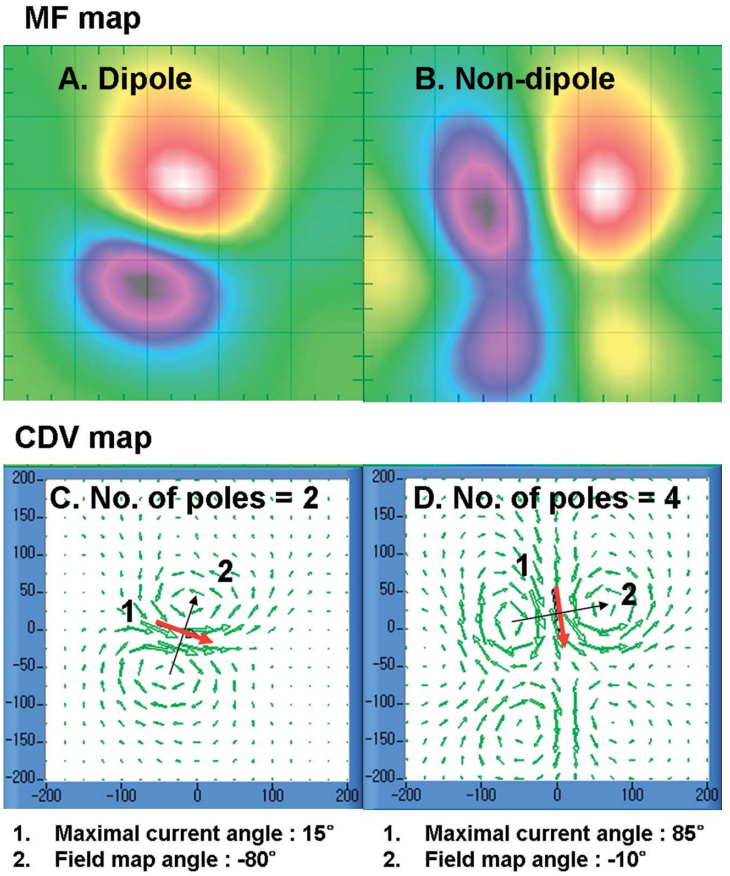

Fig 3. (A, B) Magnetic field (MF) and (C, D) current density vector (CDV) maps at distal 40 ms to Te, The patterns of dipole (A) and non-dipole (B) are shown. The number of poles is 2 and 4 in the CDV maps (C) and (D), respectively. The maximum current angle (arrow 1 in C and D) and the field map angle (arrow 2 in C and D) are shown.

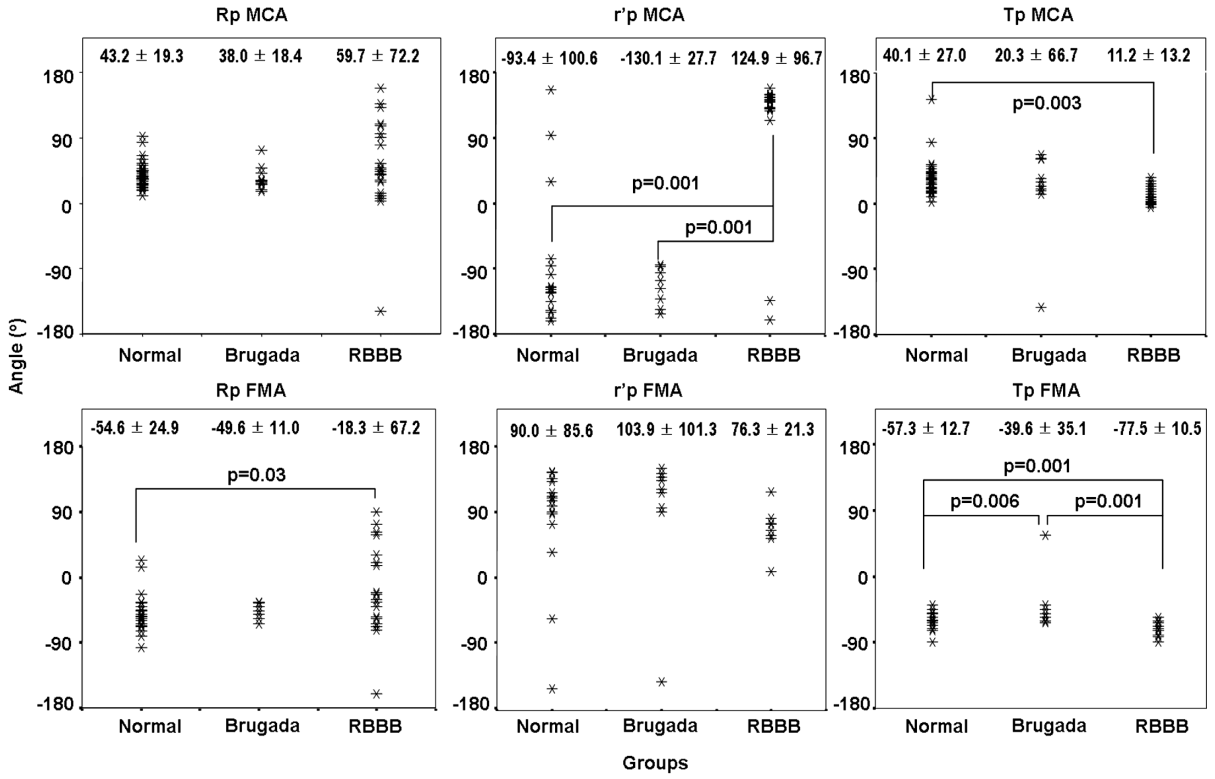

Fig 4. Comparison of the maximum current angle (MCA) and field map angle (FMA) of the R peak (Rp), r' peak (r'p), and T-wave peak (Tp). Note the MCA of the r'p falls in the northwest axis in right bundle branch block (RBBB) group, whereas it is right axis deviated in the Brugada syndrome (BS) (p=0.001) and normal groups (p=0.001).

Table 1 Comparison of the Frequency of a Non-Dipole Pattern During Late Repolarization in the Magnetic Field Map Among the 3 Groups

Time (ms)	*Non-dipole (n)/total (n)*			*p value between*		
	Brugada	*RBBB*	*Normal*	*Brugada-RBBB*	*Brugada-normal*	*RBBB-normal*
Te	*10/10*	*21/21*	*34/34*	–	–	–
Te-10	*10/10*	*16/21*	*33/34*	*0.09*	*1.0*	*0.03*
Te-20	*9/10*	*14/21*	*19/34*	*0.06*	*0.07*	*1.0*
Te-30	*9/10*	*6/21*	*11/34*	*0.001*	*0.02*	*1.0*
Te-40	*9/10*	*4/21*	*4/34*	*0.001*	*0.001*	*0.46*
Te-50	*9/10*	*4/21*	*3/33*	*0.001*	*0.001*	*0.41*
Te-60	*8/10*	*4/21*	*3/32*	*0.002*	*0.001*	*0.42*

RBBB, right bundle branch block; Te, end of the T wave.

Table 2 Comparison of the Number of Poles During the Repolarization in the Current Density Vector Map Among the 3 Groups

Time (ms)	*No. of poles (n)*			*p value between*		
	Brugada	*RBBB*	*Normal*	*Brugada-RBBB*	*Brugada-normal*	*RBBB-normal*
Te	*5.5±1.1*	*4.7±1.0*	*3.9±0.8*	*0.03*	*0.001*	*0.03*
Te-10	*5.1±1.2*	*4.1±1.1*	*3.3±0.8*	*0.01*	*0.001*	*0.006*
Te-20	*4.7±1.2*	*3.1±1.0*	*2.6±0.6*	*0.001*	*0.001*	*0.06*
Te-30	*4.3±1.3*	*2.7±0.7*	*2.4±0.5*	*0.001*	*0.001*	*0.18*
Te-40	*3.8±1.0*	*2.4±0.5*	*2.2±0.3*	*0.001*	*0.001*	*0.25*
Te-50	*3.5±0.8*	*2.3±0.5*	*2.1±0.3*	*0.001*	*0.001*	*0.29*
Te-60	*3.1±0.7*	*2.5±0.5*	*2.1±0.4*	*0.001*	*0.001*	*0.35*

Abbreviations see in Table 1.

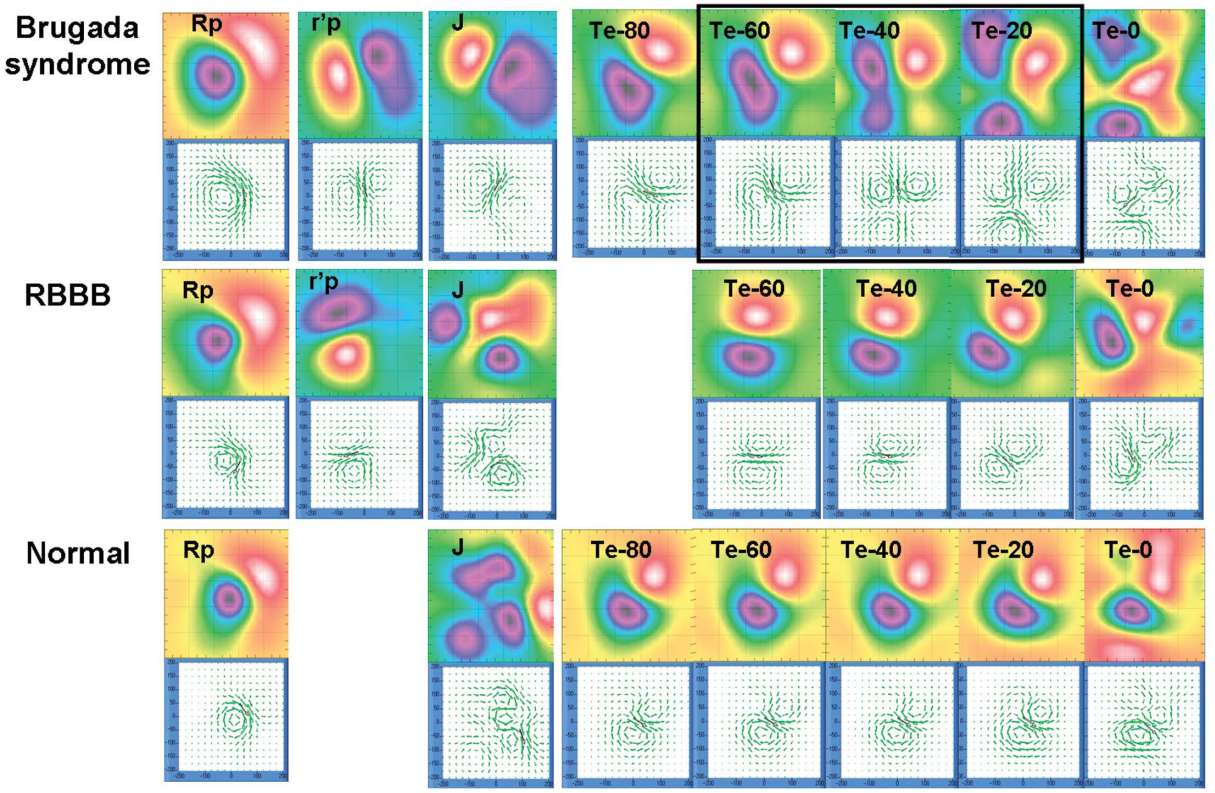

Fig 5. Comparison of the MF and CDV maps during depolarization and repolarization among the 3 groups. In the MF maps during the repolarization, a non-dipole pattern is more common in the BS group than in the RBBB or normal group. Also in the CDV maps during repolarization, the number of poles is higher in the BS group than in the RBBB and normal groups (box). See Figs 3, 4 for abbreviations. Te, end of the Twave.

vectors of the magnetic current around heart. The MF map is a color-coded image of the CDV map. In the MF map, the red and blue poles represent outgoing magnetic fields and inward fields with respect to the plane of the thorax, respectively. The analyses of MF and CDV maps were performed from Te back to Tp. The pattern of the poles was defined as dipole when there were 2 poles (Fig 3A) and as non-dipole when there were more than 2 poles (Fig 3B). In the CDV map, the number of poles was counted (Figs 3C,D). Briefly, this classification system is based on the notion that, during normal repolarization, the underlying electrical activity will be coordinated and that the current distributions represented in the MF and CDV maps will be primarily characterized by currents in a left and downward direction. Disturbances in repolarization will affect the symmetry of the maps. The maximum current and field map angles were calculated at R peak (Rp), r' peak (r'p), and T-wave peak (Tp). The maximum current angle was almost the same angle as the angle of the electrical conduction which is tangential to the field map angle (arrow 1 in Fig 3C). The field map angle represented the angle of a line connecting the negative blue pole to the positive red pole in the MF map (arrow 2 in Fig 3C).

Data Analysis

The differences in the amplitudes of Rp, r'p and Tp, maximum current and MF map angles were compared among the patient groups using an ANOVA test. The differences in the non-dipole pattern between the patient groups were compared using a chi-square test. The differences in the number of poles among the patient groups were estimated using an ANOVA test. A p-value <0.05 was considered to be significant.

Results

Comparison of MCG Time Tracings and STAG Among the 3 Groups

The QT and Tp to Te intervals measured in the integrated MCG time tracings did not differ among the groups (data not presented). The MF strength of the Rp was 232.4±123.0, 362.3±139.7 and 296.1±115.1 nA.m in the BS, RBBB and normal groups, respectively. The BS group had a lower amplitude of Rp than did the RBBB group (p=0.007). The r' wave belonged to the noise range and was too small to interpret in 1 (10%) BS and 17 (50%) normal patients. The MF strength of the r' was 143.8±50.5, 200.4±97.2 and 132.2±54.4 nA.m in the BS, RBBB and normal groups, respectively. The RBBB group had a higher amplitude of the r' than did the normal group (p=0.009).

In the comparison of the STAG from depolarization to repolarization, the activation of the r' wave was more prominent in the RBBB group than in the normal group (Fig 2). With the horizontal STAG, r' waves were located on the neural side in 7 of 9 (78.8%) BS patients and in 14 of 17 (82.4%) normal patients compared with on the right side in all RBBB patients (21 of 21, 100%). The r' waves were more frequently located on the right side in the RBBB group than in the normal (p=0.001) or BS groups (p=0.001).

Comparison of the Maximum Current and Field Map Angles Among the 3 Groups

The maximum current angle of the r'p was –130.1±

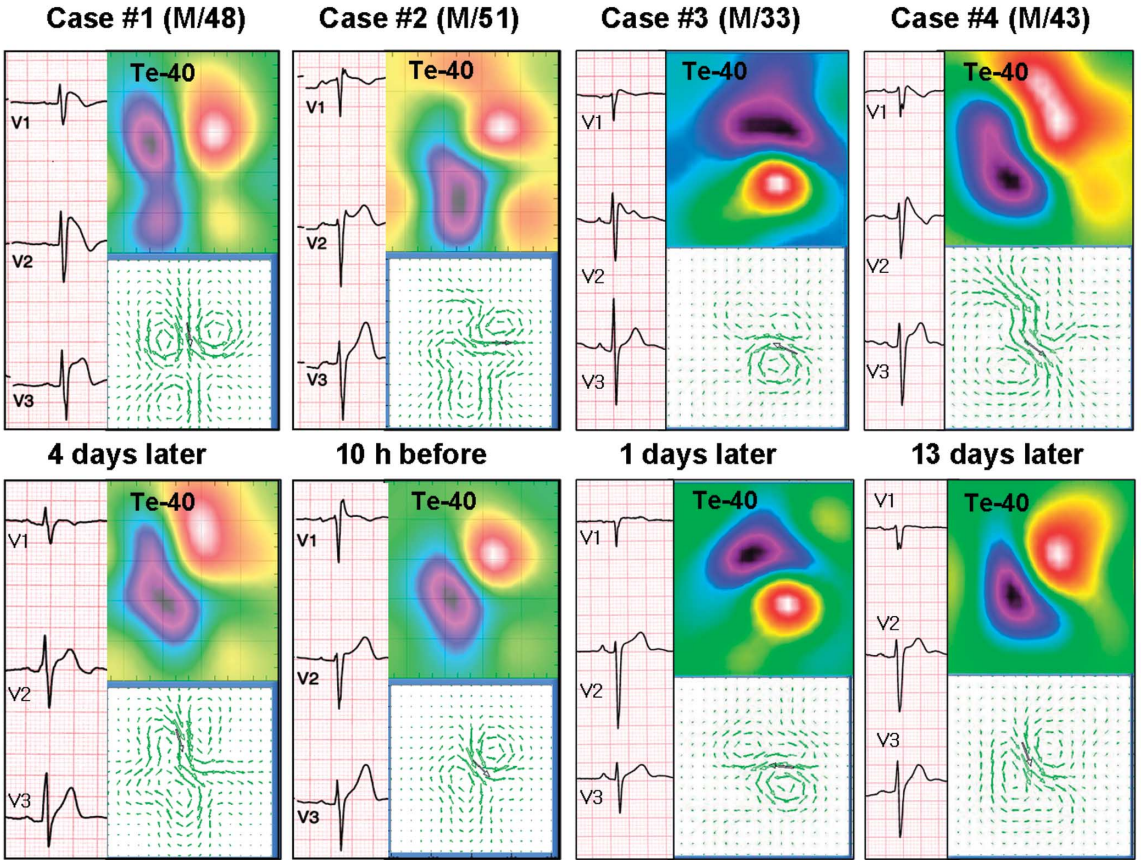

Fig 6. Change in the magnetic dispersion pattern of the late repolarization in the magnetic field (MF) and current density vector (CDV) maps with variable electrocardiographic (ECG) changes in Brugada syndrome. (Upper and lower panels) ECG and corresponding MF and CDV maps of each patient (see text for details). Te, end of the Twave.

27.7°, 124.9±96.7° and –93.4±100.6° in the BS, RBBB and normal groups, respectively. The r'p was too small to measure the maximum current angle in 1 (10%) BS and 17 (50%) normal patients. Of note, the maximum current angles of the r'p fell into the northwest axis in all 9 BS patients as compared with a right axis deviation in 19 of 21 (90.4%) RBBB patients (p=0.001, Fig 4).

Comparison of Non-Dipole Pattern and the Number of Poles Among the 3 Groups

In the MF map, the number of patients with a non-dipole pattern was higher in the BS group than in the RBBB (p=0.001) or normal (p=0.001, Table 1) groups during the last 60 ms and 40 ms to the Te. In the comparison of the number of poles during late repolarization on the CDV map, the BS patients had more poles than did the RBBB and normal patients, especially between the last 60–20 ms to the Te (Table 2, Fig 5).

Change in the Magnetic Dispersion in Accordance With the ECG Pattern in BS Patients

In 9 BS patients, the MCG was recorded more than twice. However, MCG recording during the different types of BS ECGs was possible to obtain in 4 BS patients. The magnetic dispersion of late repolarization also changed with the variable ECG changes in the same BS patients.

The 1st panel on the left in Fig 6 shows the ECG and MCG findings in a 48-year-old BS patient (case #1). In the upper panel, the patient exhibits a coved-type ST-segment elevation on the ECG, a non-dipole pattern on the MF maps and a pole number of 4 on the CDV maps. Four days after the appearance of the saddle-back-type ST-segment elevation, the ECG of the same patient was almost normal, except in V_1 there was a non-dipole and a lesser pole number of 2 on the MF and CDV maps recorded in the last 40 ms to the Te. The 2nd panel of Fig 6 shows the ECG and MCG findings for a 51-year-old BS patient (case #2). In the upper panel, the patient exhibits a saddle-back-type ST-segment elevation in the ECG, a non-dipole pattern on the MF maps and a pole number of 3 on the CDV maps. Ten hours earlier than the appearance of the saddle-back-type ST-segment elevation, the ECG in the same patient was almost normal, and there was a dipole pattern and a pole number of 2 on the MF and CDV maps recorded in the last 40 ms to the Te. The 3rd panel of Fig 6 shows the ECG and MCG findings for a 33-year-old BS patient (case #3). In the upper panel, the patient exhibits a coved-type ST-segment elevation in the ECG, a non-dipole pattern on the MF maps and a pole number of 3 on the CDV maps. One day after the appearance of the saddle-back-type ST-segment elevation, the ECG of the same patients was normal, there was a dipole pattern and a pole number of 2 on the MF and CDV maps recorded in the last 40 ms to the Te. The right panel of Fig 6 shows the ECG and MCG findings for a 43-year-old BS patient (case #4). In the upper panel, the patient exhibits a saddle-back-type ST-segment elevation in the ECG, a non-dipole pattern on the MF maps and a pole number of 3 on the CDV maps. However, 13 days after the

appearance of the saddle-back-type ST-segment elevation, the ECG of the same patient was normal, and there was a dipole pattern and a pole number of 2 on the MF and CDV maps recorded in the last 40 ms to the Te.

Discussion

The diagnosis of BS is based on the typical ECG features: (1) an accentuated J wave appearing principally in the right precordial leads (V_{1-3}) and taking the form of an ST-segment elevation, often followed by a negative T wave; (2) very closely coupled extrasystoles; and (3) rapid polymorphic VT, which at times may be indistinguishable from VF. The ST-segment elevation may also display a saddleback appearance[11] and the VT in rare cases may be monomorphic[12] ST-segment elevation is associated with a wide variety of benign, as well as malignant, pathophysiologic conditions. A differential diagnosis is at times difficult, particularly when the degree of ST-segment elevation is relatively small. Moreover, the ECG signature of BS is dynamic and often concealed, but can be unmasked by potent sodium-channel blockers such as flecainide, ajmaline, procainamide, disopyramide, propafenone, and pilsicainide[13,14]

MCG is a new tool to record the magnetic field that exists around an electrical current. Because the 64-channel MCG system can measure the magnetic field at 64 sites simultaneously, it is possible to evaluate cardiac activation with a higher resolution than conventional ECG. Moreover, it could create MF and CDV maps every 1 ms with a very high temporal resolution.

In the MCG time tracings, a more prominent r' wave was found in patients with RBBB and BS, as with ECG. The magnetic field strength of the r'p was higher in the RBBB group than in the BS patients. Also in the STAG analysis, we found a more prominent r'p. Using the whole-heart electrical-activation diagram (W-HEAD) model, Kandori et al[6] visualized the spatial time-variant activation in the whole heart. They mainly described the activation of R-peak and showed a posteromedian left ventricle excitation in BS with half the amplitude of RBBB, and a low electrical conduction rate to the posterosuperior septum area. Contrary to the W-HEAD model, which shows horizontal and anterior to posterior time-variant cardiac activation[6] our STAG analysis provided both the longitudinal and horizontal cardiac activation according to time. In this study, we could not find a difference in the activation of the R-peak. The only prominent different finding between the RBBB and other groups was observed during r'p in the horizontal STAG. The r'p in all of the RBBB patients was located on the right side. Therefore, we could easily differentiate RBBB from BS and normal with the horizontal STAG analysis.

In the MF and CDV maps, BS demonstrated a characteristic magnetic dispersion of late repolarization. The magnetic dispersion during the ST-T interval has been reported in patients with coronary heart disease[15] An interesting finding was the variation of the magnetic dispersion of the late repolarization in association with the temporal ECG changes in the same BS patient. Although our serial MCG data from the same patient was limited, the magnetic dispersion pattern of the repolarization appeared to be more prominent in the coved-type ECGs than in the saddle-back and normal type ECG patterns. One of the main explanations for malignant arrhythmias is based on regional inhomogeneity of the refractory periods of the myocardial cells, despite a constant heart rate. The electrophysiological background reflects the different duration of the monophasic action potentials and a delayed occurrence of some action potentials because of the slow conduction properties[16,17]

Study Limitations

Because of the limited number of BS patients, it may not be possible to give final conclusions about the MCG findings in BS. However, this study has merit as a pioneer study. Although we did not record MCG and 12-lead ECG simultaneously, the 2 recordings were taken within 30 min of each other. However, we can not exclude the possibility of transient change during this period. If we performed a provocation test for BS patients before and after MCG recording, it might be possible to present more data about the changes according to the different types of BS ECG changes[18] To study the MCG findings of BS patients with minimal clinical manifestation will be needed to show the additional role of MCG in the diagnosis of BS patients.

Conclusion

Using MCG, the horizontal STAG location and maximum current angle of the r' wave are beneficial in differentiating BS from RBBB and normal during depolarization. The magnetic dispersion was a more frequently observed finding in BS than in RBBB and normal during late repolarization.

References

1. Brugada P, Brugada J. Right bundle branch block, persistent ST-segment elevation and sudden cardiac death. *J Am Coll Cardiol* 1992; **20:** 1391–1396.
2. Antzelevitch C, Brugada P, Brugada J, Brugada R, Shimizu W, Gussak I, et al. Brugada syndrome: A decade of progress. *Circ Res* 2002; **91:** 1114–1118.
3. Yan GX, Antzelevitch C. Cellular basis for the Brugada syndrome and other mechanisms of arrhythmogenesis associated with ST segment elevation. *Circulation* 1999; **100:** 1660–1666.
4. Morita H, Fukushima-Kusano K, Nagase S, Takenaka-Morita S, Nishii N, Kakishita M, et al. Site-specific arrhythmogenesis in patients with Brugada syndrome. *J Cardiovasc Electrophysiol* 2003; **14:** 373–379.
5. Kandori A, Shimizu W, Yokokawa M, Maruo T, Kanzaki H, Nakatani S, et al. Detection of spatial repolarization abnormalities in patients with LQT1 and LQT2 forms of congenital long-QT syndrome. *Physiol Meas* 2002; **23:** 603–614.
6. Kandori A, Miyashita T, Ogata K, Shimizu W, Yokokawa M, Kamakura S, et al. Electrical space-time abnormalities of ventricular depolarization in patients with Brugada syndrome and patients with complete right-bundle branch blocks studied by magnetocardiography. *Pacing Clin Electrophysiol* 2006; **29:** 15–20.
7. Nakazawa K, Sakurai T, Kishi R, Takagi A, Osada K, Ryu S, et al. Discrimination of Brugada syndrome patients from individuals with the saddle-back type ST-segment elevation using a marker of the standard 12-lead electrocardiography. *Circ J* 2007; **71:** 546–549.
8. Wilde AA, Antzelevitch C, Borggrefe M, Brugada J, Brugada R, Brugada P, et al. Study group on the molecular basis of arrhythmias of the European Society of Cardiology. *Eur Heart J* 2002; **23:** 1648–1654.
9. Lee YH, Kwon H, Kim JM, Park YK, Park JC. Double relaxation oscillation SQUID with high flux-to-voltage transfer and its application to a biomagnetic multichannel system. *J Korean Phys Soc* 1998; **32:** 600–605.
10. Kim K, Lee YH, Kwon H, Kim JM, Park YK, Kim IS. Correction in the principal component elimination method for neuromagnetic-evoked field measurements. *J Korean Phys Soc* 2004; **44:** 980–986.
11. Miyazaki T, Mitamura H, Miyoshi S, Soejima K, Aizawa Y, Ogawa S. Autonomic and antiarrhythmic drug modulation of ST segment elevation in patients with Brugada syndrome. *J Am Coll Cardiol* 1996; **27:** 1061–1070.
12. Shimada M, Miyazaki T, Miyoshi S, Soejima K, Hori S, Mitamura

H, et al. Sustained monomorphic ventricular tachycardia in a patient with Brugada syndrome. *Jpn Circ J* 1996; **60:** 364–370.
13. Brugada R, Brugada J, Antzelevitch C, Kirsch GE, Potenza D, Towbin JA, et al. Sodium channel blockers identify risk for sudden death in patients with ST-segment elevation and right bundle branch block but structurally normal hearts. *Circulation* 2000; **101:** 510–515.
14. Antzelevitch C. The Brugada syndrome: Ionic basis and arrhythmia mechanisms. *J Cardiovasc Electrophysiol* 2001; **12:** 268–272.
15. Hailer B, Chaikovsky I, Auth-eisernitz S, Schafer H, Van Leeuwen P. The value of magnetocardiography in patients with and without relevant stenoses of the coronary arteries using an unshielded system. *Pacing Clin Electrophysiol* 2005; **28:** 8–16.
16. Han J, Moe GK. Non-uniform recovery of excitability in ventricular muscle. *Circ Res* 1964; **14:** 44–60.
17. Antzelevitch C, Fish J. Cardiac heterogeneity: Electrical heterogeneity within the ventricular wall. *Basic Res Cardiol* 2001; **96:** 517–527.
18. Ueyama T, Shimizu A, Yamagata T, Esato M, Ohmura M, Yoshiga Y, et al. Different effect of the pure Na^+ channel-blocker pilsicainide on the ST-segment response in the right precordial leads in patients with normal left ventricular function. *Circ J* 2007 **71:** 57–62.